

TTP 97-03<sup>1</sup>  
February 1997  
hep-ph/9702245

# The Static Potential in QCD – a full Two-Loop Calculation\*

Markus Peter

*Institut für Theoretische Teilchenphysik,  
Universität Karlsruhe  
D-76128 Karlsruhe, Germany*

February 4, 1997  
revised May 16, 1997

## Abstract

A full analytic calculation of the two-loop diagrams contributing to the static potential in QCD is presented in detail. Using a renormalization group improvement, the “three-loop” potential in momentum space is thus derived and the third coefficient of the  $\beta$ -function for the  $V$ -scheme is given. The Fourier transformation to position space is then performed, and the result is briefly discussed.

## 1 Introduction

The famous Coulomb potential of electrodynamics is very important as an essential ingredient in any non-relativistic problem involving charged particles and consequently as being responsible for many phenomena in everyday life. It is thus no surprise that its analogue in chromodynamics has also been of great interest since 20 years. Although the QCD potential certainly is not as ubiquitous in the macroscopic world, it still represents a fundamental concept which, besides the fact that potential models have been astonishingly successful in the description of quarkonia, might give us some deeper understanding of non-abelian theories and especially of confinement. There is,

---

\*Work supported in part by Graduiertenkolleg “Elementarteilchenphysik an Beschleunigern”, by the “Landesgraduiertenförderung” at the University of Karlsruhe, and by BMBF under contract 057KA92P.

<sup>1</sup> The complete paper, including figures, is also available via anonymous ftp at [ttx2.physik.uni-karlsruhe.de](ftp://ttx2.physik.uni-karlsruhe.de) (129.13.102.139) as [/ttp97-03/ttp97-03.ps](ftp://ttx2.physik.uni-karlsruhe.de/ttp97-03/ttp97-03.ps), or via www at <http://www-ttx.physik.uni-karlsruhe.de/cgi-bin/preprints>.

of course, no known way to analytically derive the confining part of the potential from first principles up to now, and consequently this paper will also be restricted to an analysis of the perturbative part. Nevertheless one may hope to obtain some hints on the non-perturbative regime in this way. In addition, a calculation of the perturbative potential is required for comparisons between continuum QCD and lattice results.

The first investigations of the interaction energy between an infinitely heavy quark-antiquark pair date back to 1977 [1, 2, 3] and were initiated by L. Susskind's Les Houches lectures [1]. In these works some general properties of the static potential were discussed and the one-loop and parts of the higher-order diagrams were computed. In the years that followed, much effort went into deriving (quark-mass suppressed) spin- and velocity-dependent corrections in various frameworks, but it is surprising that for a very long time there was no complete two-loop calculation of the true static case available. Only recently has this gap been closed [4], and the present paper is essentially an extended version of [4] presenting details about the two-loop calculation, which might be of interest for other problems as well.

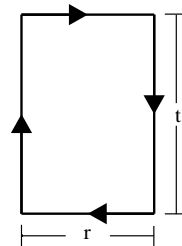
Before turning to the real problem, however, a brief description of the structure of the paper should not be missing: as an introduction of the notation and for illustrative purposes, the QED potential is discussed in section 2, which is followed by a section describing the main additional problems encountered in the non-abelian theory. Section 4 is concerned with the techniques needed for the actual two-loop calculation, and finally sections 5 and 6 contain the result for the potential in momentum and position space, respectively.

## 2 Abelian case: the QED potential

A definition of the static potential in QED which is both convenient for analytical and lattice calculations and which in addition is manifestly gauge invariant can be given as follows:

consider the vacuum expectation value of a rectangular Wilson loop of spatial extent  $r$  and temporal extent  $t$ ,

$$\langle 0 | T \exp \{ i e \oint dx_\mu A^\mu \} | 0 \rangle.$$



If we let  $t$  approach infinity, the lines corresponding to  $|t| = \infty$  will only give a negligible contribution to the line integral because the length of the integration path is much

smaller than that of the other two lines<sup>2</sup>. In other words,

$$\begin{aligned} & \langle 0 | T \exp \{ i e \oint dx_\mu A^\mu \} | 0 \rangle \\ & \xrightarrow{t \rightarrow \infty} \langle 0 | T \exp \{ i e \int_{-t/2}^{t/2} d\tau (A_0(\tau, -\mathbf{r}/2) - A_0(\tau, \mathbf{r}/2)) \} | 0 \rangle. \end{aligned}$$

The path integral representation of the remaining expectation value equals the partition function of a system described by the usual (purely photonic) QED Lagrangian with the addition of a source term  $J_\mu(x)A^\mu(x)$  with

$$J_\mu(x) = e v_\mu \left[ \delta^{(3)}\left(\mathbf{x} + \frac{\mathbf{r}}{2}\right) - \delta^{(3)}\left(\mathbf{x} - \frac{\mathbf{r}}{2}\right) \right]; \quad v_\mu \equiv \delta_{\mu 0}.$$

As the partition function is dominated by the ground state energy in this limit, i.e. the path integral approaches  $\exp(-itE_0(r))$ , and as the ground state energy is exactly what we would term the potential, we are led to define

$$V(r) = - \lim_{t \rightarrow \infty} \frac{1}{it} \ln \langle 0 | T \exp \{ i e \oint dx_\mu A^\mu \} | 0 \rangle. \quad (1)$$

For pure QED the vacuum expectation value is a gaussian path integral and an exact calculation is therefore possible, with the result

$$V(r) = e^2 \int \frac{d^3q}{(2\pi)^3} \left( \frac{1}{\mathbf{q}^2} - \frac{e^{i\mathbf{q}\mathbf{r}}}{\mathbf{q}^2} \right) = \Sigma + V_{\text{Coul.}} \quad (2)$$

where as the second term the expected Coulomb potential appears, but there is also an infinite constant representing the self-energy of the sources known from classical electrodynamics.

An exact solution will no longer be possible as soon as light fermions are included or a non-abelian theory is considered. It is therefore useful to perform a perturbative analysis as well. The Feynman rules for the sources can be read off easily: each source-photon vertex corresponds to a factor  $iev^\mu$ , an anti-source obtains an additional minus sign. When we expand the time-ordered exponential, we may introduce  $\Theta$ -function to express the different possible time-orderings of the fields  $A^\mu$ , and in turn can re-interpret them as source propagators in position space,

$$S_F(x - x') = -i\Theta(x_0 - x'_0)\delta^{(3)}(\mathbf{x} - \mathbf{x}'), \quad (3)$$

the reverse time ordering must be used for the anti-source. Transforming the expression to momentum space one obtains

$$S_F(p) = \frac{1}{vp + i\varepsilon} \quad (4)$$

---

<sup>2</sup>It should be evident from the definition (1) that a small contribution from these two lines would indeed not affect the potential.

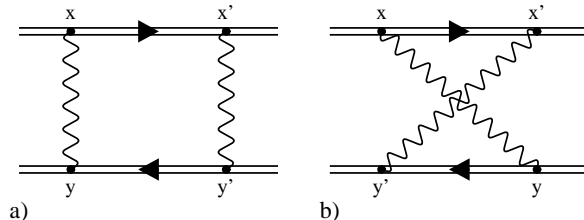


Figure 1: One-loop ladder diagrams. The double-lines represent the static sources.

with  $v \rightarrow -v$  for the anti-source. One should note that in the path-integral approach we could in fact omit the time-ordering prescription, as it is already implicit in that formalism, but the final integrals we would encounter would not be easier to solve. The approach we take, however, will prove to be very useful in the non-abelian theory.

In addition, an immediate observation is that the Feynman rules are exactly the same as those of Heavy Electron Effective Theory, the QED analogue of HQET, where  $v$  would represent the electron's velocity. This comes as no surprise, as we are investigating the infinite mass limit of QED, and it is well known that the potential can also be derived from the scattering operator. The static QED potential thus should be derivable from the scattering matrix of HEET, correspondingly the QCD potential from HQET, and this is in fact what is done in practice. This approach can even be used to determine the spin-dependent corrections to the potential [6].

At tree level, one obtains the scattering amplitude

$$-ie^2 \int dx_0 dy_0 v_\mu v_\nu D^{\mu\nu}(x-y) \Big|_{\mathbf{x}=0, \mathbf{y}=\mathbf{r}} = -ie^2 t \int \frac{d^3 q}{(2\pi)^3} \frac{e^{i\mathbf{q}\mathbf{r}}}{-\mathbf{q}^2}$$

where  $D^{\mu\nu}$  is the photon propagator. At first glance this seems to be the complete result already and one might wonder what happens with the higher order diagrams. But some care is required because the sum of all diagrams does not correspond to the potential, but to its exponential. That is exactly what the loop graphs are needed for. At one-loop order for example, the ladder diagrams shown in Fig. 1 appear. When working in position space it is easy to see that summing the two effectively removes the anti-source propagator — because it is only a  $\Theta$ -function. Hence, adding them once more with  $x \leftrightarrow x'$  the source propagator is also removed and one finds

$$2! \times \text{Fig. 1} = \left( -ie^2 t \int dx_0 dy_0 D^{00}(x-y) \Big|_{\mathbf{x}=0, \mathbf{y}=\mathbf{r}} \right)^2.$$

(A similar analysis in momentum space is also feasible, but more difficult [4].) It is clear from the way the ladder diagrams are constructed that this behaviour persists to all orders: the ladder diagrams are derived from the uncrossed ladder by permuting all vertices, i.e. generating all time-orderings, on one of the two fermion lines. Hence after

summing all of them we end up with the uncrossed ladder again, where the  $\Theta$ -functions on one of the fermion lines are removed. The source propagators on the other line are removed by adding the same sums, with all possible permutations of the names of the vertices, just as was done in the one-loop example. Since there are  $n!$  permutations at  $n$ -loops, the exponential thus forms.

The other types of graphs — source self-energy and vertex correction diagrams — can be shown, along the same line, to produce the products of the form  $\Sigma^n \cdot V_{\text{Coul.}}^m(r)$  predicted by the exact formula (2).

If light fermions are to be included, an explicit exact expression for the potential can no longer be derived and one has to rely on the perturbative treatment. The effect of the fermions is to introduce a running coupling in two different ways. The obvious point is that fermion loops cause vacuum polarization effects, which can be accounted for by defining an effective charge in momentum space via

$$\alpha_{\text{eff}}(\mathbf{q}^2) = \frac{\alpha}{1 + \Pi(\mathbf{q}^2)}$$

where  $\Pi(\mathbf{q}^2)$  represents the vacuum polarization function and  $\alpha$  the fine structure constant. This definition is gauge invariant and includes a Dyson summation. One might thus guess that

$$V(\mathbf{q}^2) = -\frac{4\pi\alpha_{\text{eff}}(\mathbf{q}^2)}{\mathbf{q}^2}, \quad (5)$$

but the formula need only be correct at the one- and two-loop level, because starting at three loops light-by-light scattering diagrams enter. The correct formula should read

$$V(\mathbf{q}^2) = -\frac{4\pi\alpha_v(\mathbf{q}^2)}{\mathbf{q}^2}, \quad (6)$$

with  $\alpha_v \neq \alpha_{\text{eff}}$ , which, however, merely serves as a definition of  $\alpha_v$ . Nevertheless, this definition is quite convenient, especially when turning to the non-abelian case where a gauge-invariant definition of an effective charge is nontrivial.

### 3 Complications in the non-abelian case

One novelty that arises in QCD is well known: the non-linear nature of non-abelian theories introduces additional diagrams which cause a running coupling even in the absence of light fermions, and the fact that gluons carry colour also requires a redefinition of the Wilson loop and consequently of the potential as follows:

$$V(r) = -\lim_{t \rightarrow \infty} \frac{1}{it} \ln \langle 0 | \text{Tr P exp} \left( ig \oint dx_\mu A_a^\mu T^a \right) | 0 \rangle. \quad (7)$$

The generators  $T^a$  have to be inserted in order to absorb the gluons' colour index, and the fact that the generators do not commute requires the introduction of a path-ordering prescription. An important point is that this prescription is not automatically taken into account by using the path-integral formalism, in contrast to the time-ordering. Consequently, all we can do even in the path-integral approach is use the definition of the path-ordered exponential, i.e. expand it, and the usefulness of the way we analyzed the abelian case should become clearer. The net effect of the modifications in the non-abelian case is a complication of the way the exponentiation of the potential arises, and that the sources are automatically in a colour singlet state.

In principle we are free to choose any representation for the generators, but since we intend to describe quarks we are going to use the fundamental one. On tree level, the only change with respect to QED then is the colour factor  $C_F = T_F(N^2 - 1)/N$  that multiplies the coupling in the potential, where  $N$  is the number of colours and  $T_F$  the normalization of the generators. It is thus convenient to define, in analogy to (6),

$$V(\mathbf{q}^2) = -C_F \frac{4\pi\alpha_v(\mathbf{q}^2)}{\mathbf{q}^2}, \quad (8)$$

as this has the following advantage:  $C_F$  is the value of the Casimir operator  $T^a T^a = C_R \mathbf{1}$  in the fundamental representation  $T_{ij}^a = \lambda_{ij}^a/2$ , where the  $\lambda^a$  are the Gell-Mann matrices. If we chose the adjoint representation  $T_{ij}^a = -if^{aij}$ , which would be equally acceptable, the only thing that would change in (8) is the overall factor  $C_F$  which would be replaced by  $C_A$ , the coupling  $\alpha_v$  would remain the same. The statement is trivial at tree level, but it is in fact true to all orders as will be explained after the discussion on the exponentiation. By choosing the adjoint representation we obtain the static potential for gluinos in a colour singlet state.

In higher orders the presence of the generators causes the individual diagrams to obtain different colour factors and consequently the exponentiation has to be more involved than in the abelian case. Although this point has already been analyzed in [2], it seems appropriate to recall the discussion here. It should, however, suffice to consider the ladder diagrams to explain the basic idea.

The QCD one-loop ladder diagrams corresponding to Fig. 1 obtain the colour factors

$$\text{Fig. 1a} \propto C_F^2 \quad , \quad \text{Fig. 1b} \propto C_F^2 - \frac{C_A}{2} C_F \quad (9)$$

and we immediately can identify the abelian-like terms  $\propto C_F^2$  that are needed to build the exponential of the Coulomb potential. But it is also obvious that the remainder of Fig. 1b, together with a contribution from the vertex corrections involving the same colour factor, gives an additional contribution to the potential, which then has to be exponentiated by the higher order diagrams.

Fig. 2 shows the two-loop ladder diagrams, which involve the colour factors

$$\text{Fig. 2a} \quad \propto C_F^3 \quad (10)$$

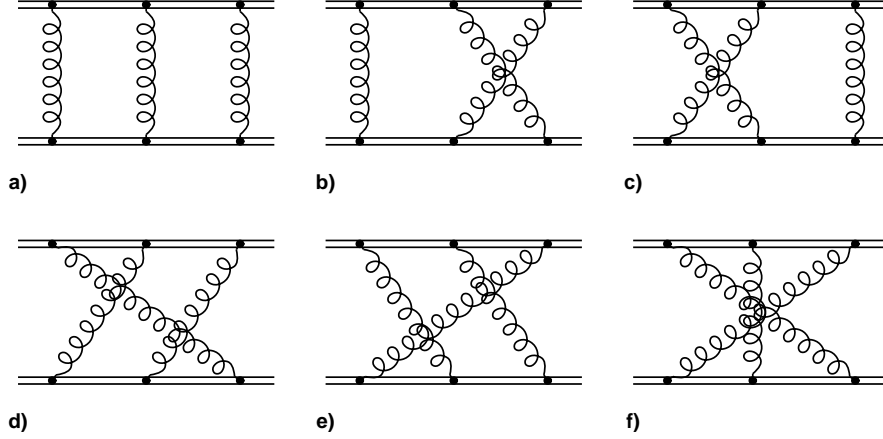


Figure 2: Two-loop ladder diagrams in QCD.

$$\text{Fig. 2b, c} \propto C_F^3 - C_F^2 \frac{C_A}{2} \quad (11)$$

$$\text{Fig. 2d, e} \propto C_F^3 - 2C_F^2 \frac{C_A}{2} + \frac{C_A^2}{4} C_F \quad (12)$$

$$\text{Fig. 2f} \propto C_F^3 - 3C_F^2 \frac{C_A}{2} + \frac{C_A^2}{2} C_F. \quad (13)$$

As expected, each diagram contains the “abelian” term  $C_F^3$ , thus forming an iteration of the tree-level potential, but the terms  $\propto C_F^2 C_A$  are also iterations, exactly those that arise from exponentiating the additional one-loop term. This can be seen as follows: when working in coordinate space and neglecting the colour factors, we can look for combinations of the diagrams in which one of the anti-source propagators is removed, with the result

$$\begin{aligned} (b) + (e) + (f) &= \text{Diagram with vertical gluon on left and gluon loop on right} \\ (c) + (d) + (f) &= \text{Diagram with gluon loop on left and vertical gluon on right} \\ (d) + (e) + (f) &= \text{Diagram with gluon loop on left and gluon loop on right} \end{aligned}$$

Summing the three lines we find that the coefficients of  $-C_F^2 C_A/2$  in Eqs. (11–13) equal the corresponding diagrams’ coefficients in the sum and that the  $\Theta$ -functions

fixing the position of the marked gluon line are removed. Hence the sum is a product of one-gluon exchange and the crossed ladder diagram with exactly the right colour factor. A similar analysis for the remaining two-loop diagrams leads to the conclusion that the exponentiation works in the non-abelian case as well, and that all terms  $\propto C_F^3$  or  $C_F^2 C_A$  indeed constitute iterations.

In consequence, the number of diagrams that really have to be computed to determine the two-loop contribution to the QCD potential is somewhat reduced. Nevertheless, when compared to QED the number of diagrams is still quite large, as in the abelian case only very few remain (essentially the vacuum polarization).

Having discussed the exponentiation we are able to prove the statement that  $\alpha_v$  is independent of the representation the sources are in. It is obvious that for any representation  $R$ , the colour factor for a given diagram is the same as the one for  $R = F$  if we replace  $C_F$  by  $C_R$ , because it is completely determined by the algebra of the generators: only  $C_R$  and  $C_A$  can appear since the generators themselves and the structure constants arising from commutators are the only “matrices” around, and their combination is fixed. We have also seen that at each loop order the only net contribution to the potential arises from the colour factors linear in  $C_F$ , all other terms are iterations. The definition (8) then implies that  $\alpha_v$  does not involve  $C_F$  at all<sup>3</sup> and thus the replacement  $C_F \rightarrow C_R$  does not affect the coupling.

## 4 Details of the two-loop calculation

It is worth presenting at least some details of the techniques used to compute the two-loop diagrams, first of all because they are helpful when trying to reproduce the results, but also because they might prove useful for other calculations as well.

The remaining diagrams are best analyzed in momentum space, using the kinematics that follows from the Wilson loop definition: the “on-shell condition” for the source reads  $vp = 0$  where  $p$  denotes the four-momentum carried by the source. Thus the sources may have any three-momenta, the actual values of which are, however, unimportant, as the only quantity that appears is the momentum transfer  $q^\mu = (0, \mathbf{q})$ .

By choosing a convenient gauge the number of graphs can be further reduced: if we employ Feynman gauge, all diagrams with a three- or four gluon vertex with all gluons directly coupled to source lines vanish. This welcome feature is caused by the replacement of the Dirac matrices  $\gamma^\mu$  in the source-gluon vertex by the simple factor  $v^\mu = \delta^{\mu 0}$ , which means that all vertices are interchangeable as far as their Lorentz structure and momentum dependence is concerned (the momentum dependence is mentioned because

---

<sup>3</sup>We only consider factors  $C_F$  coming from the sources here. Of course  $\alpha_v$  does involve  $C_F$ , but these terms arise from fermion loops and are unrelated to the representation of the external sources. Consequently they should not be replaced.



it is the property which is destroyed by other gauges). The symmetry properties of both the three- and four gluon vertices then imply that the diagrams vanish.

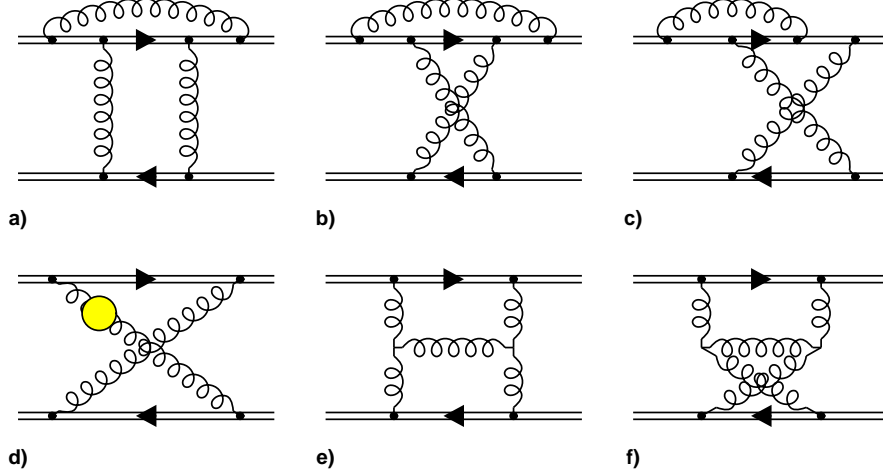


Figure 3: Two-gluon exchange diagrams in QCD that remain in Feynman gauge.

Consequently, apart from the ladders Fig. 2d–f, the two-loop gluon self-energy and double insertions of one-loop corrections, only a few of the two-loop vertex correction graphs and the six two-gluon exchange diagrams of Fig. 3 have to be calculated. In fact the number of diagrams is even slightly lower because Fig. 3f has a vanishing colour factor for sources in the colour singlet state, and of the ladder diagrams only Fig. 2f is required, because the relation

$$\text{Fig. 2d} + 2\text{e} = -\text{Fig. 2f} \quad (14)$$

holds if the corresponding colour factors are neglected. The equality can easily be proven in momentum space by applying the trivial identity

$$\frac{1}{lv - kv + i\varepsilon} \frac{1}{kv + i\varepsilon} - \frac{1}{lv - kv + i\varepsilon} \frac{1}{lv + i\varepsilon} = \frac{1}{kv + i\varepsilon} \frac{1}{lv + i\varepsilon}$$

to one of the two source lines.

Using dimensional regularization with  $D = 4 - 2\varepsilon$  for both the infrared and ultraviolet divergencies, the integration by parts technique [7] can be used to reduce most of the integrals that arise to products or convolutions of four types of one-loop integrals, that in turn can be computed by standard methods. With the notation

$$\begin{aligned} \widetilde{d}p &\equiv \frac{(2\pi\mu)^{2\varepsilon}}{i\pi^2} d^D p \quad , \quad \mathcal{P}_n(p) \equiv p^{\mu_1} p^{\mu_2} \dots p^{\mu_n} , \\ G(n, m; k, j) &= (4\pi\mu^2)^\varepsilon \frac{\Gamma(n + m - j - \frac{D}{2})}{\Gamma(n)\Gamma(m)} B\left(\frac{D}{2} - n + k - j, \frac{D}{2} - m + j\right), \end{aligned} \quad (15)$$

$$G_H(n, m; k, j) = (4\pi\mu^2)^\epsilon \frac{\Gamma(\frac{D}{2} - n + k - j)\Gamma(2n + m - k - D)}{\Gamma(n)\Gamma(m)} \quad (16)$$

the integrals are, omitting the  $i\epsilon$  in the propagators for brevity:

$$\begin{aligned} & \int \widetilde{d}p \left( \frac{1}{-p^2} \right)^n \left( \frac{1}{-(p-q)^2} \right)^m \mathcal{P}_k(p) \\ &= (-q^2)^{D/2-n-m} \sum_{j=0}^{[k/2]} G(n, m; k, j) \left( \frac{q^2}{4} \right)^j \frac{1}{j!} \left( \frac{\partial}{\partial q_\mu} \frac{\partial}{\partial q^\mu} \right)^j \mathcal{P}_k(q), \end{aligned} \quad (17)$$

$$\begin{aligned} & \int \widetilde{d}p \left( \frac{1}{-p^2} \right)^n \left( \frac{w}{pv+w} \right)^m \mathcal{P}_k(p) \\ &= (-1)^k (-2w)^{D+k-2n} \sum_{j=0}^{[k/2]} G_H(n, m; k, j) \left( \frac{-1}{4} \right)^j \left( \frac{\partial}{\partial v_\mu} \frac{\partial}{\partial v^\mu} \right)^j \mathcal{P}_k(v), \end{aligned} \quad (18)$$

$$\begin{aligned} & \int \widetilde{d}p \left( \frac{1}{-p^2} \right)^n \left( \frac{1}{-(p-q)^2} \right)^m \left( \frac{1}{-pv} \right)^a \Big|_{vq=0} \\ &= (-q^2)^{\frac{D-a}{2}-n-m} \frac{\sqrt{\pi}}{\Gamma(\frac{a+1}{2})} G(n, m; -a, -a/2), \end{aligned} \quad (19)$$

$$\begin{aligned} & \int \widetilde{d}p \left( \frac{1}{-p^2} \right)^n \left( \frac{w}{pv+w} \right)^a \left( \frac{w}{pv} \right)^b \\ &= (-2w)^{D-2n} \frac{\Gamma(D-2n-b)}{\Gamma(D-2n)} G_H(n, a; -b, -b). \end{aligned} \quad (20)$$

The formula for the standard massless two-point function Eq. (17) is a well known result which can be found for example in [7]. Its HQET analogue (18) and the HQET three-point functions (19) and (20) can be calculated in a similar way using the parametrization

$$\frac{1}{a^n b^m} = \frac{\Gamma(n+m)}{\Gamma(n)\Gamma(m)} \int_0^\infty d\alpha \frac{\alpha^{m-1}}{(a+\alpha b)^{n+m}}$$

to combine gluon and source propagators, instead of the usual Feynman parameters. Eq. (18) without the factor  $\mathcal{P}_k(p)$  has already been given in [8], and Eq. (20) can be derived from Eq. (8) of [9].

The reduction of a given graph to the two functions  $G$  and  $G_H$  can be automated with the help of a computer program such as FORM [10], but an additional final reduction to a few basic  $G_{(H)}$ -functions seems quite difficult because of the appearance of  $\epsilon$ -dependent values for the last two arguments of  $G$  and  $G_H$  and additional ratios of  $\Gamma$ -functions. As an example consider the integral

$$\begin{aligned} & \int \widetilde{d}p \widetilde{d}p' \frac{1}{p^2(p+q)^2(p')^2(p'v)^2(p'v+pv)(pv)} \\ & \stackrel{(20)}{=} -\frac{2^{D-2}\Gamma(D-4)}{\Gamma(D-2)} G_H(1, 1; -2, -2) \int \widetilde{d}p \frac{1}{(-p^2)(-(p+q)^2)(-pv)^{6-D}} \end{aligned}$$

$$\stackrel{(19)}{=} \frac{-8\Gamma(-2\epsilon)\Gamma(1+\epsilon)}{\Gamma(2-2\epsilon)\Gamma(2+2\epsilon)} G_H(1, 1; -2, -2) G(1, 1; -2-2\epsilon, -1-\epsilon) (-q^2)^{-1-2\epsilon}$$

which corresponds to Fig. 3b. It thus seems easier to directly rewrite the resulting expressions in terms of  $\Gamma$ -functions and immediately expand them in  $\epsilon$ .

However, as already mentioned, not all of the graphs can be reduced in an easy way to the above one-loop integrals, a few diagrams remain that involve the following type of true two-loop integrals:

$$I(a, b, c; n, m) = \int \widetilde{d}p \widetilde{d}r \left(\frac{-1}{p^2}\right)^a \left(\frac{-1}{r^2}\right)^b \left(\frac{-1}{(p-r-q)^2}\right)^c \frac{1}{(pv)^n} \frac{1}{(rv)^m} \quad (21)$$

with  $vq = 0$  and  $n, m > 0$ . From

$$\int \widetilde{d}p \widetilde{d}r v_\mu \frac{\partial}{\partial p_\mu} f(p, r; q) = 0$$

one can derive the recursion relation

$$nN^+I = 2(aA^+ + cC^+)N^-I - 2cC^+M^-I. \quad (22)$$

Here the operator  $N^+$  means that the argument  $n$  of  $I$  should be increased by one, and correspondingly for the other operators. The relation can be used to reduce integrals with  $n > 1$  or  $m > 1$  to those with  $n = m = 1$ . For example, with  $n = 1, m = 2$  we find for the integral corresponding to Fig. 2f:

$$I(1, 1, 1; 2, 2) = 2I(2, 1, 1; 0, 2) + 2I(1, 1, 2; 0, 2) - 2I(1, 1, 2; 1, 1). \quad (23)$$

The first two terms can be computed with the help of (17)–(20), but the last one cannot be simplified any further by the recursion relation (due to the absence of the propagators  $1/(p-q)^2$  and  $1/(r-q)^2$  there are no other simple relations).

It turns out that the following three “irreducible” integrals, the calculation of which is sketched in the appendix, are needed:

$$I(1, 1, 1; 1, 1) = \frac{2\pi}{3} (-q^2)^{-2\epsilon} G(1, 1; -1, -\frac{1}{2}) G(1, \frac{1}{2} + \epsilon; -1, -\frac{1}{2}) \quad (24)$$

$$I(1, 1, 2; 1, 1) = -\frac{2}{q^2} \left(\frac{4\pi\mu^2}{-q^2}\right)^{2\epsilon} \left[ \frac{1}{\epsilon^2} - \frac{2}{\epsilon} + 4 - \frac{5}{6}\pi^2 - \epsilon \left( 8 - \frac{5}{3}\pi^2 + \frac{32}{3}\zeta_3 \right) + \mathcal{O}(\epsilon^2) \right] \quad (25)$$

$$I(2, 1, 2; 1, 1) = \frac{1}{(q^2)^2} \left(\frac{4\pi\mu^2}{-q^2}\right)^{2\epsilon} \left[ \frac{2}{\epsilon^2} + \frac{2}{\epsilon} - 4 - \frac{5}{3}\pi^2 - \frac{\epsilon}{3} \left( 24 - 17\pi^2 - 64\zeta_3 \right) + \mathcal{O}(\epsilon^2) \right]. \quad (26)$$

With these equations all the basic formulæ for the determination of the two-loop diagrams are given. The expressions for the individual graphs will, however, not be listed here, we will directly turn to the complete result instead.

## 5 The QCD potential in momentum space

A convenient way of writing the QCD potential in momentum space is<sup>4</sup>

$$V(\mathbf{q}^2) = -C_F \frac{4\pi\alpha_V(\mathbf{q}^2)}{\mathbf{q}^2} \quad (27)$$

$$\alpha_V(\mathbf{q}^2) = \alpha_{\overline{\text{MS}}}(\mu^2) \sum_{n=0}^{\infty} \tilde{a}_n(\mu^2/\mathbf{q}^2) \left(\frac{\alpha_{\overline{\text{MS}}}(\mu^2)}{4\pi}\right)^n \quad (28)$$

$$= \alpha_{\overline{\text{MS}}}(\mathbf{q}^2) \sum_{n=0}^{\infty} a_n \left(\frac{\alpha_{\overline{\text{MS}}}(\mathbf{q}^2)}{4\pi}\right)^n \quad (29)$$

with  $a_0 = \tilde{a}_0 = 1$  and where

$$a_1 = \frac{31}{9}C_A - \frac{20}{9}T_F n_f \quad , \quad \tilde{a}_1 = a_1 + \beta_0 \ln \frac{\mu^2}{\mathbf{q}^2} \quad (30)$$

is the long-known one-loop result and

$$a_2 = \left(\frac{4343}{162} + 6\pi^2 - \frac{\pi^4}{4} + \frac{22}{3}\zeta_3\right)C_A^2 - \left(\frac{1798}{81} + \frac{56}{3}\zeta_3\right)C_A T_F n_f \\ - \left(\frac{55}{3} - 16\zeta_3\right)C_F T_F n_f + \left(\frac{20}{9}T_F n_f\right)^2 \quad (31)$$

$$\tilde{a}_2 = a_2 + \beta_0^2 \ln^2 \frac{\mu^2}{\mathbf{q}^2} + (\beta_1 + 2\beta_0 a_1) \ln \frac{\mu^2}{\mathbf{q}^2} \quad (32)$$

is the new information added by the present analysis. Note that the last term of  $a_2$  could have been predicted from the one-loop result, it is exactly the contribution that would be Dyson-summed in QED by introducing an effective coupling. The third term originates from the two-loop vacuum polarization and thus would also be included in the effective coupling in the case of QED.

Knowledge of  $a_2$  now allows us to consistently use the three-loop expression for the running coupling in the  $\overline{\text{MS}}$ -scheme. An equation of the form (29) can then be used to derive the  $\beta$ -function of one of the two couplings from the knowledge of the  $\beta$ -function of the second scheme. If we define  $\beta$  and the coefficients  $\beta_n$  in each scheme via

$$\frac{1}{\alpha(\mu^2)} \frac{d\alpha(\mu^2)}{d \ln \mu^2} = -\beta(\alpha) = -\sum_{n=0}^{\infty} \beta_n \left(\frac{\alpha(\mu^2)}{4\pi}\right)^{n+1}, \quad (33)$$

we immediately find

$$\beta^V(\alpha_V) = \beta^{\overline{\text{MS}}}(\alpha_{\overline{\text{MS}}}) \frac{\alpha_{\overline{\text{MS}}}}{\alpha_V} \frac{d\alpha_V}{d\alpha_{\overline{\text{MS}}}} \quad \text{with } \alpha_{\overline{\text{MS}}} = \alpha_{\overline{\text{MS}}}(\alpha_V) \quad (34)$$

---

<sup>4</sup> The second and third equations might be incomplete for  $n > 2$ , because  $a_n$  might depend on  $\ln \alpha$ , see the discussion in [3]. The present paper, however, is restricted to the three-loop potential, i.e.  $n \leq 2$ .

or  $\beta_{0,1}^V = \beta_{0,1}^{\overline{\text{MS}}}$  and

$$\begin{aligned}
\beta_2^V &= \beta_2^{\overline{\text{MS}}} - a_1 \beta_1^{\overline{\text{MS}}} + (a_2 - a_1^2) \beta_0^{\overline{\text{MS}}} & (35) \\
&= \left( \frac{618 + 242\zeta_3}{9} + \frac{11(24\pi^2 - \pi^4)}{12} \right) C_A^3 \\
&\quad - \left( \frac{445 + 704\zeta_3}{9} + \frac{24\pi^2 - \pi^4}{3} \right) C_A^2 T_F n_f \\
&\quad + \frac{2 + 224\zeta_3}{9} C_A (T_F n_f)^2 - \frac{686 - 528\zeta_3}{9} C_A C_F T_F n_f \\
&\quad + 2C_F^2 T_F n_f + \frac{184 - 192\zeta_3}{9} C_F (T_F n_f)^2. & (36)
\end{aligned}$$

Inserting the numbers one finds that the numerical value of  $\beta_2^V$  is considerably larger than that of  $\beta_2^{\overline{\text{MS}}}$ , which, for comparison, is given by the expression [11]

$$\begin{aligned}
\beta_2^{\overline{\text{MS}}} &= \frac{2857}{54} C_A^3 + 2C_F^2 T_F n_f - \frac{205}{9} C_A C_F T_F n_f - \frac{1415}{27} C_A^2 T_F n_f \\
&\quad + \frac{44}{9} C_F (T_F n_f)^2 + \frac{158}{27} C_A (T_F n_f)^2. & (37)
\end{aligned}$$

Hence the coupling in the potential runs faster than the  $\overline{\text{MS}}$ -coupling.

Figure 4 compares the result for  $\alpha_v$  at the various loop-orders in graphical form, neglecting quark thresholds for simplicity: the dotted line represents the tree-level prediction, i.e. a pure Coulomb potential without a running coupling; the dashed line shows the one-loop result in the sense that only the (one-loop) running of  $\alpha_{\overline{\text{MS}}}$  is taken into account, but the two couplings still coincide (which means that it is still tree level as far as the diagrams contributing to the potential are concerned and should thus better be termed leading order); the dashed-dotted line shows the next-to-leading order and the solid line the next-to-next-to-leading order results. It is evident that the two-loop contribution is nearly as important as the one-loop effect: the additional shift in  $\alpha_v$  caused by  $a_2$  is roughly two third the size of the shift introduced by  $a_1$ , and both corrections increase the coupling. The impact of this shift on the would-be toponium system, as an example, should be measurable: in the interval  $|\mathbf{q}| = 10 \dots 30\text{GeV}$  including the NNLO-corrections amounts to a net increase of  $\alpha_v$  by about 5 to 7%. The charmonium and bottomonium systems on the other hand are mainly sensitive to momenta below 2GeV and thus lie predominantly outside of the perturbative domain.

At this point we should mention that for simplicity we have chosen a fixed number of five light flavours to be valid over the whole range of momenta. For a more realistic study, the bottom and charm quark thresholds would, of course, have to be taken into account by matching effective theories with decreasing  $n_f$  in order to restore decoupling. Such a procedure would, however, leave our results qualitatively unchanged, it would mainly cause an even faster running of both couplings at low momenta.

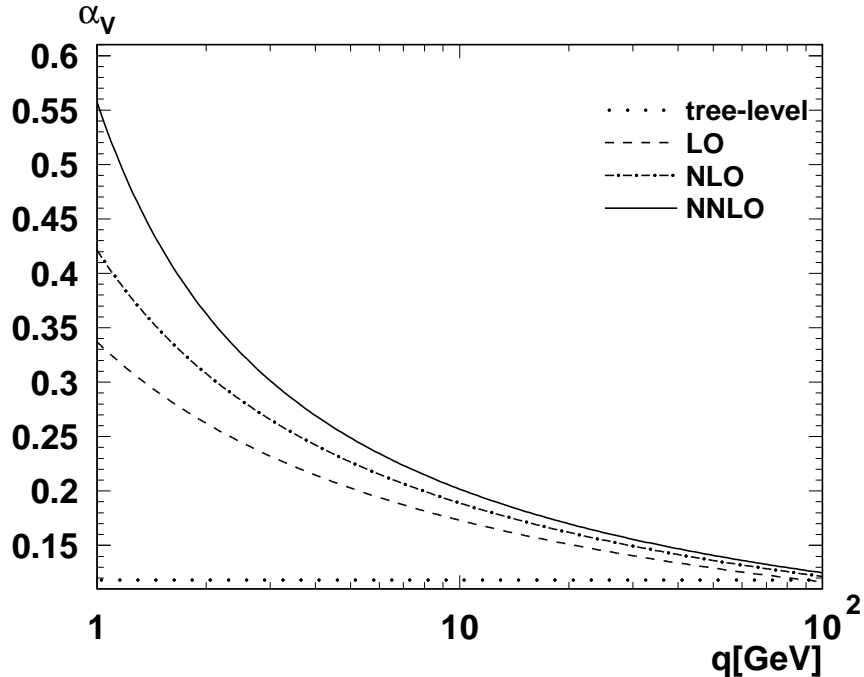


Figure 4: Comparison of the results for  $\alpha_V(\mathbf{q}^2)$  at different loop-orders, where  $\alpha_V(\mathbf{q}^2)$  is determined from  $\alpha_{\overline{\text{MS}}}(\mathbf{q}^2)$ . Input parameters are  $\alpha_{\overline{\text{MS}}}(M_Z^2) = 0.118$ ,  $n_f = 5$ .

The plot just discussed was generated by employing (29) as it stands, i.e. by evolving the  $\overline{\text{MS}}$ -coupling, taken to equal 0.118 at the  $Z$ -mass, to the required scale (assuming  $n_f = 5$ ) and then calculating  $\alpha_V$  at that scale. In principle the evolution can be performed in different ways: one may express the coupling in terms of the QCD scale parameter  $\Lambda_{\text{QCD}}$ , or one may employ the QED-like formula

$$\frac{\alpha(\mu^2)}{\alpha(q^2)} = 1 + \frac{\alpha(\mu^2)}{4\pi} \beta_0 \ln \frac{q^2}{\mu^2} + \left(\frac{\alpha(\mu^2)}{4\pi}\right)^2 \beta_1 \ln \frac{q^2}{\mu^2} + \left(\frac{\alpha(\mu^2)}{4\pi}\right)^3 \left(\beta_2 \ln \frac{q^2}{\mu^2} - \frac{1}{2} \beta_0 \beta_1 \ln^2 \frac{q^2}{\mu^2}\right). \quad (38)$$

Although the two approaches are formally equivalent, in practice only the second one guarantees that the running coupling really coincides with its input value  $\alpha(\mu^2)$  for  $q^2 = \mu^2$ . Therefore the second approach has been adopted throughout this paper.

One may argue that to first evolve the  $\overline{\text{MS}}$ -coupling and then determine the potential is not the best idea because, as is evident from Fig. 4, the expansion parameter becomes large at low scales and thus the next terms of the perturbation series might also become important. An alternative would be to determine  $\alpha_V$  from (29) at the  $Z$ -mass and then evolve it to the scale  $\mathbf{q}^2$ . It turns out, not surprisingly, that the result is essentially the

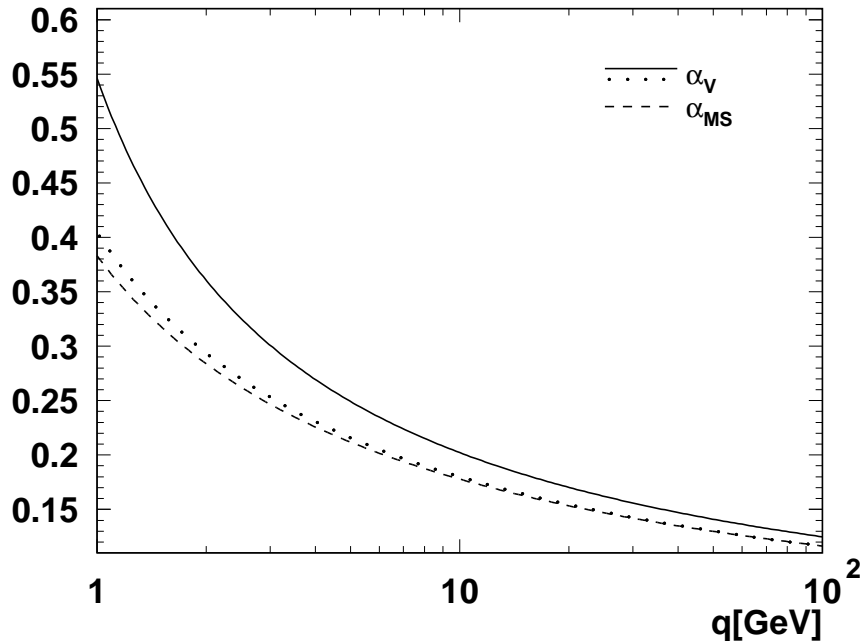


Figure 5: Comparison of the running of  $\alpha_V(\mathbf{q}^2)$  (solid line) and  $\alpha_{\overline{\text{MS}}}(\mathbf{q}^2)$  (dashed line) at three loops. The dotted curve displays  $\alpha_V(\mathbf{q}^2)$  with the initial value  $\alpha_V(M_Z^2) = \alpha_{\overline{\text{MS}}}(M_Z^2)$

same, as can be seen from Figure 5 where the running of the two couplings is compared: the solid line shows the three-loop running of  $\alpha_V$  and the dashed one  $\alpha_{\overline{\text{MS}}}$ , again for  $\alpha_{\overline{\text{MS}}}(M_Z^2) = 0.118$  and five flavours; the dotted line shows the corresponding result for  $\alpha_V$  for the hypothetical case  $\alpha_V(M_Z^2) = 0.118$  as well, and thus really displays the different  $\beta$ -functions. It exemplifies that the large numerical mismatch between the two couplings at low scales mainly arises from an amplification of the small mismatch at large scales. Note that in a sense the two couplings are the same at the two-loop level as the  $\beta$ -functions then coincide and a difference merely arises because the evolutions start at different values.

## 6 Position space

With the momentum-space representation of  $V_{\text{QCD}}$  at our disposal, we are able to compute the real analogue of the Coulomb potential, i.e. the QCD potential in position space. In order to make the expressions simpler, it is convenient to introduce the

notation

$$\mathcal{F}(r, \mu, u) = \mu^{2u} \int \frac{d^3q}{(2\pi)^3} \frac{e^{i\mathbf{q}\mathbf{r}}}{(\mathbf{q}^2)^{1+u}} \quad (39)$$

for the Fourier transform of a general power of  $1/\mathbf{q}^2$ . Using a Schwinger parameter,

$$\frac{1}{(\mathbf{q}^2)^{1+u}} = \frac{1}{\Gamma(1+u)} \int_0^\infty dx x^u e^{-x\mathbf{q}^2},$$

and a few relations between  $\Gamma$ -functions such as

$$\Gamma(1+u) = \sqrt{\pi} \frac{\Gamma(1+2u)}{2^{2u}\Gamma(\frac{1}{2}+u)}, \quad \ln \Gamma(1+u) = \gamma_E u + \sum_{n=2}^\infty \frac{\zeta(n)}{n} u^n \quad \text{for } |u| < 1,$$

several equivalent representations of  $\mathcal{F}$  can be derived, two of which will be useful in the following:

$$\mathcal{F}(r, \mu, u) = \frac{(\mu r)^{2u}}{4\pi^2 r} \frac{\Gamma(\frac{1}{2}+u)\Gamma(\frac{1}{2}-u)}{\Gamma(1+2u)} \quad (40)$$

$$= \frac{(\mu r e^{\gamma_E})^{2u}}{4\pi r} \exp\left(\sum_{n=2}^\infty \frac{\zeta(n)u^n}{n} (2^n - 1 - (-1)^n)\right) \quad (41)$$

where the first formula is applicable if  $-1 < u < 1/2$ , the second if  $|u| < 1/2$  and where  $\gamma_E$  denotes the Euler-Mascheroni constant.

Adopting a strictly perturbative approach, we can use the original result leading to (27) (or in other words re-expand  $\alpha_{\overline{\text{MS}}}(\mathbf{q}^2)$ ) to find the potential in position space. From

$$\begin{aligned} \alpha_v(\mathbf{q}^2) &= \alpha_{\overline{\text{MS}}}(\mu^2) \left( 1 + \frac{\alpha_{\overline{\text{MS}}}(\mu^2)}{4\pi} \left( -\beta_0 \ln \frac{\mathbf{q}^2}{\mu^2} + a_1 \right) \right. \\ &\quad \left. + \left( \frac{\alpha_{\overline{\text{MS}}}(\mu^2)}{4\pi} \right)^2 \left( (\beta_0 \ln \frac{\mathbf{q}^2}{\mu^2})^2 - (2\beta_0 a_1 + \beta_1) \ln \frac{\mathbf{q}^2}{\mu^2} + a_2 \right) + \dots \right), \end{aligned} \quad (42)$$

where  $\mu$  is the renormalization scale, we see that we need the Fourier transform of  $\ln^m(\mu^2/\mathbf{q}^2)$  which we easily obtain from  $\mathcal{F}$  because

$$\ln^m \frac{\mu^2}{\mathbf{q}^2} = \left[ \frac{\partial^m}{\partial u^m} \left( \frac{\mu^2}{\mathbf{q}^2} \right)^u \right] \Big|_{u=0}$$

and thus

$$\int \frac{d^3q}{(2\pi)^3} \ln^m \frac{\mu^2}{\mathbf{q}^2} \frac{e^{i\mathbf{q}\mathbf{r}}}{\mathbf{q}^2} = \left( \frac{\partial^m}{\partial u^m} \mathcal{F}(r, \mu, u) \right) \Big|_{u=0}. \quad (43)$$

Hence the potential in position space becomes

$$\begin{aligned} V(r) &= -C_F \frac{\alpha_{\overline{\text{MS}}}(\mu^2)}{r} \left( 1 + \frac{\alpha_{\overline{\text{MS}}}(\mu^2)}{4\pi} (2\beta_0 \ln(\mu r') + a_1) \right. \\ &\quad \left. + \left( \frac{\alpha_{\overline{\text{MS}}}(\mu^2)}{4\pi} \right)^2 \left( \beta_0^2 (4 \ln^2(\mu r') + \frac{\pi^2}{3}) \right. \right. \\ &\quad \left. \left. + 2(\beta_1 + 2\beta_0 a_1) \ln(\mu r') + a_2 \right) + \dots \right) \end{aligned} \quad (44)$$



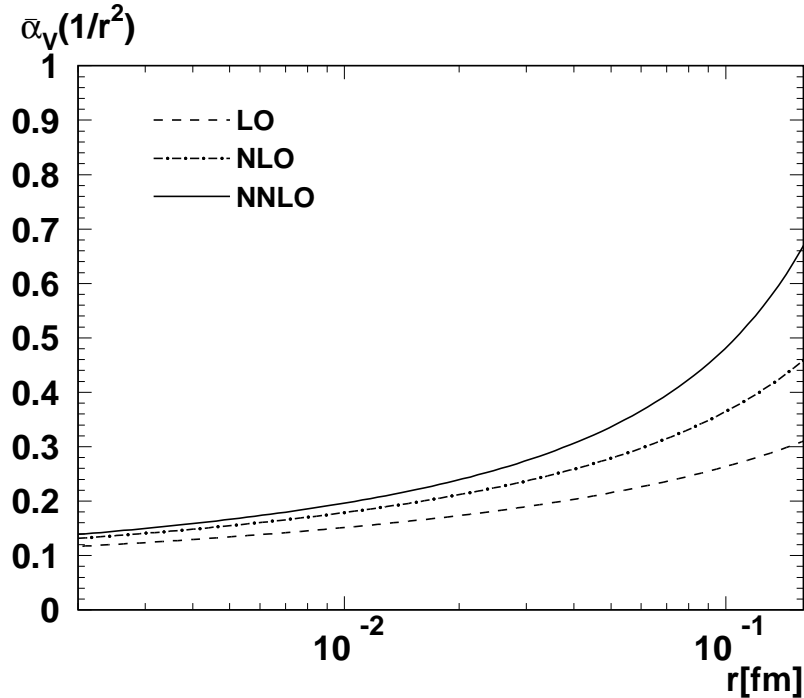


Figure 6: The potential (times  $-r/C_F$ ) in position space at different orders choosing  $\mu = 1/r$ . The range in  $r$  roughly corresponds to the range in  $|\mathbf{q}|$  displayed in the previous figures:  $r = 10^{-2.6}\text{fm} \approx 0.002\text{fm} \sim 100\text{GeV}$  and  $r = 10^{-0.8}\text{fm} \approx 0.16\text{fm} \sim 1\text{GeV}$ .

with  $r' \equiv r \exp(\gamma_E)$ . One should note that going beyond the strictly perturbative approach is quite difficult and may lead to inconsistencies as the running coupling has a pole and thus the Fourier transform of (27) does not exist. But as the pole is an artifact which arises because a perturbative expression is extrapolated deep into the non-perturbative regime, it should not be taken too seriously.

The result (44) may be exploited in several ways: we certainly would not use it as it stands because of the possibly large logarithms, but choose a scale  $\mu$  that reduces the higher order corrections. The first and in some sense natural choice is  $\mu_1 = 1/r$ , leading to the curves displayed in Fig. 6 where the effect of the loop-corrections on  $rV(r)$  is shown, using the same input parameters as before. As the tree-level prediction would correspond to a constant in this plot, it has been omitted. The graph is essentially the same as Figure 4 and therefore will not be discussed further.

A second choice motivated by noticing that due to (41),  $\mu$  will always appear in combination with  $r'$ , is  $\mu_2 = 1/r'$ . This way we remove all terms involving  $\gamma_E$  from the coefficients. Note that these terms are not small numerically because in  $n$ th order they involve  $(2\gamma_E\beta_0)^m \approx \beta_0^m$  for all  $m \leq n$  as well as similar contributions from the other

$\beta_m$ .

A third choice, which is frequently encountered in other contexts as well, would be to select  $\mu$  in such a way as to remove the first-order coefficient completely, i.e.  $\mu_3(r) = \exp[-\gamma_E - a_1/(2\beta_0)]/r$ , which leads to

$$V_3(r) = -C_F \frac{\alpha_3}{r} \left( 1 + \left( \frac{\alpha_3}{4\pi} \right)^2 \left( a_2 - a_1^2 - \frac{\beta_1}{\beta_0} a_1 + \frac{(\pi\beta_0)^2}{3} \right) \right) \quad (45)$$

with  $\alpha_3 \equiv \alpha_{\overline{\text{MS}}}(\mu_3^2(r))$ . This approach is in effect similar to defining an effective charge like in QED, but one should remember that it cannot be interpreted as a Dyson summation of the one-loop vacuum polarization and therefore there is no reason why it should constitute a superior choice. A real Dyson summation would lead to problems with gauge invariance except for some part of the fermion loop contribution.

Yet another possibility, which is similar in spirit, would be to choose  $\mu$  in such a way as to remove all  $n_f$ -dependence from the coefficients  $a_n$ , i.e. to use the BLM scale setting prescription [12]. This procedure leads to

$$V_{\text{BLM}}(r) = -\frac{C_F}{r} \left( \alpha_{\overline{\text{MS}}}\left(\frac{1}{r_1^2}\right) + a_1^{\text{BLM}} \frac{\alpha_{\overline{\text{MS}}}^2(1/r_2^2)}{4\pi} + a_2^{\text{BLM}} \frac{\alpha_{\overline{\text{MS}}}^3(1/r'^2)}{(4\pi)^2} \right) \quad (46)$$

with

$$a_1^{\text{BLM}} = -\frac{8}{3}C_A \quad (47)$$

$$a_2^{\text{BLM}} = \left( \frac{133 - 396\zeta_3}{9} + \frac{24\pi^2 - \pi^4}{4} \right) C_A^2 - \frac{385 - 528\zeta_3}{12} C_A C_F \quad (48)$$

$$r_1^2 = r'^2 e^{5/3} \quad (49)$$

$$r_2^2 = r'^2 \exp\left( \frac{434 - 504\zeta_3}{192} - \frac{315 - 432\zeta_3}{192} \frac{C_F}{C_A} \right) \approx r'^2 e^{-0.42}. \quad (50)$$

Finally, a fifth choice follows from proceeding in analogy to momentum space and defining

$$V(r) = -C_F \frac{\bar{\alpha}_V(1/r)}{r}. \quad (51)$$

From (44) one may calculate the  $\beta$ -function of the new coupling, with the result

$$\bar{\beta}_2^V = \beta_2^V + \frac{\pi^2}{3} \beta_0^3, \quad (52)$$

and, after determining the initial value for  $\bar{\alpha}_V$  at  $M_Z$  from (44) (where there are again different choices for  $\mu$  possible, we have used  $\mu = 1/r$ ) evolve it to the right distance. It is evident that the appearance of  $\gamma_E$  and the  $\zeta$ -functions makes  $\bar{\alpha}_V$  differ from  $\alpha_V$ , and consequently the same statements holds for the  $\beta$ -functions.

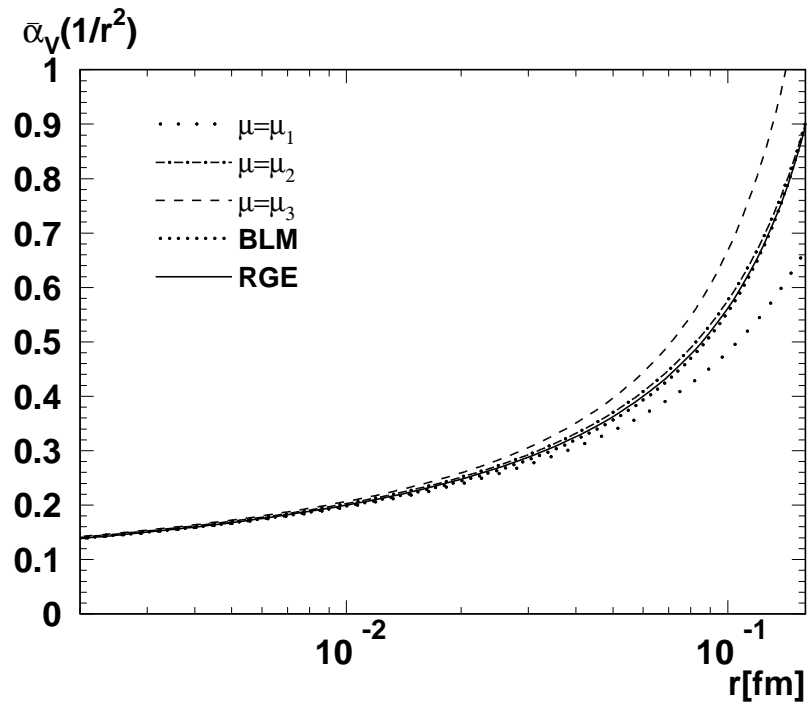


Figure 7:  $-rV(r)/C_F$  in the different schemes described in the text.

The five approaches obviously result in different predictions for the three-loop potential — the difference formally being of the order  $\alpha^4$  — as is explicitly demonstrated in Figures 7 and 8. One should note that there is no a priori reason to prefer any choice of scale. The second choice  $\mu = 1/r'$  might be an exception, as it consistently absorbs terms which only arise from the Fourier transformation and are not directly related to the dynamics. It suggests that the distance complementary to  $|\mathbf{q}|$  is not  $r$  but  $r'$ . But still “non-dynamical” terms  $\zeta_n$  remain even in this scheme. The BLM-prescription, which requires more than a single scale, is also physically motivated, and the nice agreement between the two curves and the curve resulting from the renormalization group evolution (labelled “RGE” in the figures) may serve as an argument in favour of these approaches.

The coupling  $\bar{\alpha}_V$  is already quite large at a distance  $r \sim 0.5\text{GeV}^{-1}$  or  $0.1\text{fm}$ , and its size is even strongly increased in the second and third approach due to a reduction of its scale implying that the non-perturbative regime starts at smaller separations. For five flavours for example we have  $\mu_2 \approx 0.56/r$  and  $\mu_3 \approx 0.41/r$ . As a consequence there is a large scheme-dependence of the potential in the region  $r > 0.07\text{fm}$ . From Figure 8 we see that the situation is even worse as the perturbation series must break down near  $r = 0.1\text{fm}$  because the potential starts to bend down there already. We thus should not trust the perturbative result for distances larger than about  $0.08\text{fm}$ , which is consistent with the assumption that the perturbative potential should be reliable if  $r\Lambda_{\text{QCD}} < 0.07 \dots 0.1$  is satisfied<sup>5</sup> [14, 15].

An interesting question is whether our result gives any indication on the onset of a linear rise of the potential, or in other words on the existence of confinement. Unfortunately, the situation seems unclear in this respect. As Figure 6 proves, each new term of the perturbation series that is added makes the deviation from a pure Coulomb prediction larger and the potential more attractive. But according to the conventional definition (8), a linearly *rising* potential requires a *negative* coupling, the perturbative curve for  $\bar{\alpha}_V$  thus tends into the wrong direction, and there is no sign of a nontrivial zero of this function. The only indication on the existence of a zero is the breakdown of perturbation theory at distances of the order  $r \approx 0.1\text{fm}$  (or in other words the presence of the Landau pole) and the fact that, with increasing number of loops, this point appears at smaller and smaller distances. In some sense the gap between the perturbative and the linear part thus becomes broader.

## 7 Conclusion

We have presented results of a full NNLO-calculation of the perturbative static potential in QCD both in momentum and position space, including a description of the technique employed, and we have argued that the respective couplings  $\alpha_V$  and  $\bar{\alpha}_V$  are

---

<sup>5</sup>For five flavours and  $\alpha_{\overline{\text{MS}}}(M_Z) = 0.118$  we find  $\Lambda_{\text{QCD}} \approx 210\text{MeV}$ .

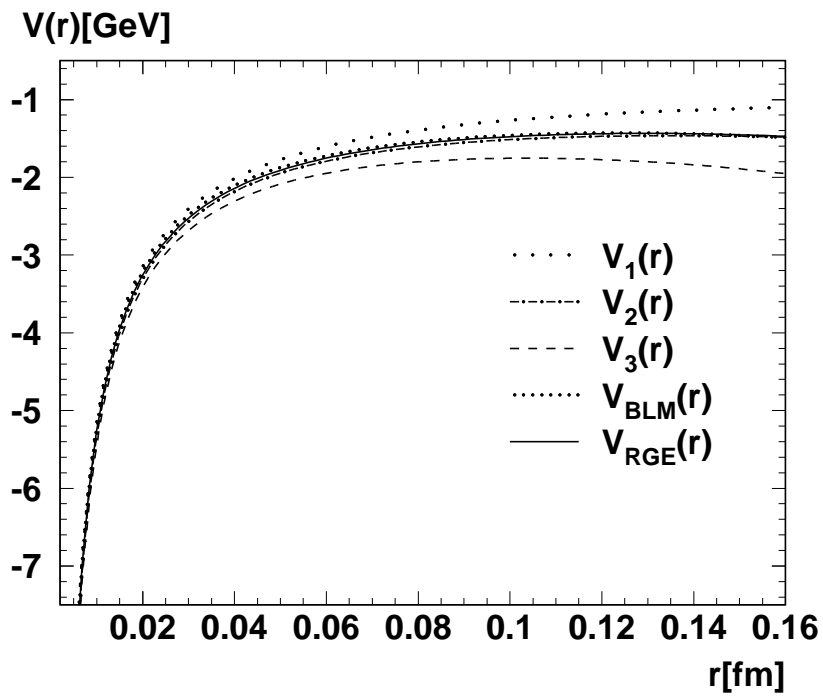


Figure 8: Three-loop potential in the different schemes described in the text.

universal in the sense that they describe the potential for other infinitely heavy colour sources such as static gluinos as well. The  $\beta$ -functions corresponding to the two couplings have been derived. The main result is that the two-loop contribution is nearly as large as the one-loop term, both make the interaction more attractive, and that the perturbative potential seems to be reasonably reliable up to distances  $r\Lambda_{\text{QCD}} < 0.07$ . For larger values a strong scale-dependence remains and the perturbation series even breaks down above about 0.1fm. Although the results may be interpreted as an indication of a general tendency of higher loop corrections to strengthen the force between a quark-antiquark pair, to take them as a proof of confinement would be going too far.

Starting from the results presented in this paper, it would be important to know, first, the impact of the two-loop contribution to the potential as a whole and, second, of the ambiguity due to different choices of scale on the energy levels and decay widths of quarkonia. The first point could be investigated in the toponium system as this is only sensitive to very short distances and does not suffer from the uncertainties arising from intermediate and large separations. The second point, however, would require the specification of some potential model for the latter region and thus the analysis would depend on additional parameters. Nevertheless, a revised study of the type performed in [15] would be very interesting.

## Acknowledgments

The author would like to thank Prof. J. H. Kühn for carefully reading the manuscript and his continuous comments and advice, and Prof. Th. Mannel for many interesting discussions.

## Appendix: Calculation of the two-loop integrals

When trying to compute the two-loop integrals  $I(a, b, c; 1, 1)$ , it is convenient to combine gluon propagators using the standard formula for Feynman parameters and to combine gluon and source propagators using the modified version

$$\frac{1}{a^m b^n} = \frac{\Gamma(n+m)}{\Gamma(n)\Gamma(m)} \int_0^\infty d\alpha \frac{\alpha^{m-1}}{(a\alpha + b)^{n+m}}.$$

With this technique the two momentum integrations can be performed one after the other, and after some rescalings of the  $\alpha$ -parameters one is left with

$$I(a, b, c; 1, 1) = (4\pi\mu^2)^{2\epsilon} (-q^2)^{D-\Sigma} \frac{2\Gamma(\Sigma-D)}{\Gamma(a)\Gamma(b)\Gamma(c)} \tilde{I}(a, b, c) \quad (53)$$

where  $\Sigma = a + b + c + 1$  and

$$\tilde{I}(a, b, c) = 2 \frac{\Gamma(\Sigma+1-D)}{\Gamma(\Sigma-D)} \int_0^1 dx dy \int_0^\infty d\alpha d\beta x^{\frac{D}{2}-b-2} (1-x)^{\frac{D}{2}-c-1}$$

$$\times y^{b+c-\frac{D}{2}-1}(1-y)^{a-1} \left[ (\alpha + \beta)^2 + \alpha^2 \frac{1-x}{xy} + y(1-y) \right]^{D+1-\Sigma}.$$

Making the change of variables  $\alpha = u\rho$  and  $\beta = (1-u)\rho$ , the two integrations corresponding to  $\alpha$  and  $\beta$  can be done, with the result

$$\tilde{I} = \int_0^1 dx dy x^{\frac{D-3}{2}-b}(1-x)^{\frac{D-3}{2}-c} y^{\frac{D-3}{2}-a} (1-y)^{D-2-b-c} \arctan \sqrt{\frac{1-x}{xy}}. \quad (54)$$

The presence of the arctan-function makes it impossible (at least for the author) to compute the remaining integral exactly for all values of  $a, b, c$  and  $\epsilon = (4-D)/2$ . Hence only the cases really needed and only the expansion in  $\epsilon$  to the order required were treated.

For  $I(1, 1, 1; 1, 1)$  this task is quite straightforward as  $\tilde{I}(1, 1, 1)$  is in fact finite in the limit  $\epsilon \rightarrow 0$  and its expansion in  $\epsilon$  can be computed without encountering any problems. But it should be noted that due to (53)  $\tilde{I}$  must be multiplied by  $1/\epsilon$  to obtain  $I$  and thus the latter integral is divergent. It should also be mentioned that the result quoted in section 4 has not been derived in the way just described, but by constructing an equation involving the integral. This method will be explained at the end of the appendix.

The problem with the other two integrals  $\tilde{I}$  is that they do not exist if we take  $\epsilon = 0$  and that it is difficult to factor out the divergence. As a first step in this direction the substitution

$$x = \frac{1}{1+t^2y}$$

can be applied to turn (54) into

$$\tilde{I}(i, 1, 2) = \int_0^\infty dt t^{-2-2\epsilon} \arctan t \cdot K_i(t^2) \quad (55)$$

with

$$\begin{aligned} K_1(t^2) &= \int_0^1 dy y^{-1-2\epsilon} (1-y)^{-1-2\epsilon} (1+t^2y)^{2\epsilon} \\ &= \frac{\Gamma^2(-2\epsilon)}{\Gamma(-4\epsilon)} F(-2\epsilon, -2\epsilon, -4\epsilon; -t^2) \\ K_2(t^2) &= \int_0^1 dy y^{-2-2\epsilon} (1-y)^{-1-2\epsilon} (1+t^2y)^{2\epsilon} \\ &= \frac{\Gamma(-2\epsilon)\Gamma(-1-2\epsilon)}{\Gamma(-4\epsilon)} F(-2\epsilon, -1-2\epsilon, -1-4\epsilon; -t^2) \end{aligned}$$

and where  $F(a, b, c; x)$  denotes the hypergeometric function. Although this result may look quite impractical, it in fact helps: one factor  $1/\epsilon$  has been factored out, and the

expansion of the two hypergeometric functions is also possible up to terms which are not needed anyhow. Let us first examine  $K_1$ :

$$\begin{aligned}
& F(-2\epsilon, -2\epsilon, -4\epsilon; x) \\
&= 1 - \epsilon \sum_{n=1}^{\infty} \left( \prod_{j=1}^{n-1} \frac{(j-2\epsilon)^2}{j-4\epsilon} \right) \frac{x^n}{n!} = 1 - \epsilon \sum_{n=1}^{\infty} \left( \prod_{j=1}^{n-1} (j + \mathcal{O}(\epsilon^2)) \right) \frac{x^n}{n!} \\
&= 1 - \epsilon \sum_{n=1}^{\infty} \frac{x^n}{n} + \mathcal{O}(\epsilon^3) = 1 + \epsilon \ln(1-x) + \mathcal{O}(\epsilon^3).
\end{aligned}$$

Thus we find

$$K_1(t^2) = 1 + \epsilon \ln(1+t^2) + \mathcal{O}(\epsilon^3)k_1(t^2)$$

where the residual function  $k_1(t^2)$  is well behaved for  $t \rightarrow 0$ . A similar trick can be applied to  $K_2$  if we first employ the relation [13]

$$F(a, b, c; x) = (1-x)^{-b} F\left(b, c-a, c; \frac{x}{x-1}\right)$$

which transforms  $K_2$  into

$$K_2(t^2) = \frac{\Gamma(-2\epsilon)\Gamma(-1-2\epsilon)}{\Gamma(-4\epsilon)} (1+t^2)^{1+2\epsilon} F\left(-1-2\epsilon, -1-2\epsilon, -1-4\epsilon; \frac{t^2}{1+t^2}\right).$$

Now

$$\begin{aligned}
& F(-1-2\epsilon, -1-2\epsilon, -1-4\epsilon; x) \\
&= 1 - \frac{(1+2\epsilon)^2}{1+4\epsilon} x + \epsilon \frac{(1+2\epsilon)^2}{1+4\epsilon} \sum_{n=1}^{\infty} \left( \prod_{j=1}^{n-1} \frac{(j-2\epsilon)^2}{j-4\epsilon} \right) \frac{x^{n+1}}{(n+1)!} \\
&= 1 - \frac{(1+2\epsilon)^2}{1+4\epsilon} x + \epsilon \frac{(1+2\epsilon)^2}{1+4\epsilon} \sum_{n=1}^{\infty} \frac{x^{n+1}}{n(n+1)} + \mathcal{O}(\epsilon^3) \\
&= 1 - x + \epsilon(1-4\epsilon)x + \epsilon(1-x) \ln(1-x) + \mathcal{O}(\epsilon^3).
\end{aligned}$$

By noting that  $F(0) = 1$  and  $F(a, a, c; 1) = \Gamma(c)\Gamma(c-2a)/\Gamma^2(c-a)$  we can even improve the above expansion as  $F$  must be of the form  $F = 1 - x + \Gamma(-1-4\epsilon)/\Gamma^2(-2\epsilon)x + \phi(x)$  where  $\phi(x)$  vanishes for both  $x = 0$  and  $x = 1$ . Thus

$$K_2(t^2) = (1+t^2)^{2\epsilon} \left[ \frac{\Gamma(-2\epsilon)\Gamma(-1-2\epsilon)}{\Gamma(-1-4\epsilon)} (1 - \epsilon \ln(1+t^2)) - \frac{t^2}{1+2\epsilon} \right] + \mathcal{O}(\epsilon^3)k_2(t^2)$$

where  $k_2$  vanishes at the origin and at infinity.

With these approximate formulae for the  $K_i$  we can calculate the two missing integrals from (55) up to terms of the order  $\mathcal{O}(\epsilon^2)$ . The divergences still present can be extracted by writing

$$\int_0^{\infty} dt t^{-1-2\epsilon} f(t) = -\frac{f(0)}{2\epsilon} + \int_0^{\infty} dt t^{-1-2\epsilon} (f(t) - f(0)\Theta(1-t)) \quad (56)$$



where the function  $f(t)$  should be regular at the origin. The new integral is finite in the limit  $\epsilon \rightarrow 0$ , and consequently may be expanded. One should note that in the case of  $I(2, 1, 2)$  there is a term  $t^2(1+t^2)^{2\epsilon}$  in  $K_2$  that removes the bad behaviour of the integrand at the origin, but introduces the same kind of divergence for large  $t$ . The trivial change of variables  $t \rightarrow 1/t$  reduces this term to the above case again. It is essential that we treat the whole combination as of order 1: suppose, for example, we would expand  $t^2(1+t^2)^{2\epsilon}$ , generating  $2\epsilon t^2 \ln(1+t^2)$ . Inserted into (55) and proceeding as described this would produce an integral of the form

$$2\epsilon \int_0^\infty dt t^{-1+2\epsilon} \ln t \frac{\arctan t}{t}$$

which is not of  $\mathcal{O}(1)$  as we would assume, but of  $\mathcal{O}(1/\epsilon)$ . The term also demonstrates that it is crucial to know that the omitted functions  $k_i$  grow at most logarithmically after expansion in  $\epsilon$  and thus do not invalidate our power-counting in this parameter.

Let us now come back to  $I(1, 1, 1; 1, 1)$ . Starting from the original definition given in section 4, shifting first  $p \rightarrow p+r+q$ , using  $vq=0$  and

$$\frac{1}{(pv+rv+i\epsilon)(rv+i\epsilon)} = \frac{1}{pv+i\epsilon} \left[ \frac{1}{rv+i\epsilon} - \frac{1}{pv+rv+i\epsilon} \right]$$

and then replacing  $r \rightarrow -r$  in the first and shifting  $r \rightarrow r-p-q$  in the second term, one obtains:

$$\begin{aligned} I(1, 1, 1; 1, 1) &= \int \widetilde{dp} \widetilde{dr} \frac{1}{(-p^2)(-r^2)(-(r+p+q)^2)} \frac{1}{(pv+rv+i\epsilon)(rv+i\epsilon)} \\ &= - \int \widetilde{dp} \widetilde{dr} \frac{1}{(-p^2)(-r^2)(-(r-p-q)^2)} \frac{1}{pv+i\epsilon} \left[ \frac{1}{rv-i\epsilon} + \frac{1}{rv+i\epsilon} \right]. \end{aligned}$$

Hence

$$\begin{aligned} I(1, 1, 1; 1, 1) &= \frac{1}{3} \int \widetilde{dp} \widetilde{dr} \frac{1}{(-p^2)(-r^2)(-(r-p-q)^2)} \frac{1}{(pv+i\epsilon)} \left[ \frac{1}{rv+i\epsilon} - \frac{1}{rv-i\epsilon} \right] \\ &= -\frac{2\pi}{3} i \int \widetilde{dp} \widetilde{dr} \frac{\delta(rv)}{(-p^2)(-r^2)(-(r-p-q)^2)(pv+i\epsilon)} \\ &= \frac{2\pi}{3} i \sqrt{\pi} G(1, 1; -1, -\frac{1}{2}) \int \widetilde{dr} \frac{\delta(rv)}{(-r^2)(-(r-q)^2)^{1/2+\epsilon}}. \end{aligned}$$

In the last expression we can replace  $i\pi\delta(rv)$  by  $-1/(rv+i\epsilon)$  (due to  $vq=0$  the principal value part of the resulting integral vanishes) and use (19) again, or we can calculate the effective  $D-1$ -dimensional integral directly. Via both routes we find the result given in section 4.

## References

- [1] L. Susskind, *Coarse grained quantum chromodynamics* in R. Balian and C. H. Llewellyn Smith (eds.), *Weak and electromagnetic interactions at high energy* (North Holland, Amsterdam, 1977).
- [2] W. Fischler, Nucl. Phys. **B129**, 157 (1977).
- [3] T. Appelquist, M. Dine and I. J. Muzinich, Phys. Lett. **69B**, 231 (1977),  
T. Appelquist, M. Dine and I. J. Muzinich, Phys. Rev. **D17**, 2074 (1978).
- [4] M. Peter, Phys. Rev. Lett. **78**, 602 (1997).
- [5] A. Billoire, Physics Letters **92B**, 343 (1980).
- [6] Y. Chen, Y. Kuang and R. J. Oakes, Phys. Rev. **D52**, 264 (1995).
- [7] K. G. Chetyrkin and F. Tkachov, Nucl. Phys. **B192**, 159 (1981).
- [8] D. J. Broadhurst and A. G. Grozin, Phys. Lett. **B267**, 105 (1991).
- [9] E. Bagan, P. Ball and P. Gosdzinsky, Phys. Lett. **B301**, 249 (1993).
- [10] J. A. M. Vermaseren, *Symbolic Manipulation with FORM* (CAN, Amsterdam, 1991).
- [11] O. V. Tarasov, A. A. Vladimirov and A. Yu. Zharkov, Phys. Lett. **B93**, 429 (1980).  
S. A. Larin and J. A. M. Vermaseren, Phys. Lett. **B303**, 334 (1993).
- [12] S. J. Brodsky, G. P. Lepage and P. B. Mackenzie, Phys. Rev. **D28**, 228 (1983),  
S. J. Brodsky and H. J. Lu, Phys. Rev. **D51**, 3652 (1995).
- [13] I. S. Gradshteyn and I. M. Ryzhik, *Table of Integrals, Series and Products* (Academic Press, New York, 1965).
- [14] W. Buchmüller and S.-H. H. Tye, *Phys. Rev.* **D24**, 132 (1981).
- [15] K. Hagiwara, A. D. Martin and A. W. Peacock, *Z. Phys.* **C33**, 135 (1986).